

Drug Screen Targeted at Plasmodium Liver Stages Identifies a Potent Multistage Antimalarial Drug

Journal Article**Author(s):**

da Cruz, Filipa P.; Martin, Cecilie; Buchholz, Kathrin; Lafuente-Monasterio, Maria J.; Rodrigues, Tiago; Sonnichsen, Birte; Moreira, Rui; Gamo, Francisco-Javier; Marti, Matthias; Mota, Maria M.; Hannus, Michael; Prudencio, Miguel

Publication date:

2012-04

Permanent link:

<https://doi.org/10.3929/ethz-b-000047522>

Rights / license:

[Creative Commons Attribution-NonCommercial 3.0 Unported](#)

Originally published in:

The Journal of Infectious Diseases 205(8), <https://doi.org/10.1093/infdis/jis184>

Drug Screen Targeted at *Plasmodium* Liver Stages Identifies a Potent Multistage Antimalarial Drug

Filipa P. da Cruz,¹ Cécilie Martin,² Kathrin Buchholz,³ Maria J. Lafuente-Monasterio,⁴ Tiago Rodrigues,⁵ Birte Sönnichsen,² Rui Moreira,⁶ Francisco-Javier Gamo,⁴ Matthias Marti,³ Maria M. Mota,¹ Michael Hannus,² and Miguel Prudêncio¹

¹Instituto de Medicina Molecular, Faculdade de Medicina, Universidade de Lisboa, Portugal, and ²Cenix BioScience GmbH, Dresden, Germany; ³Department of Immunology and Infectious Diseases, Harvard School of Public Health, Boston, Massachusetts; ⁴Tres Cantos Medicine Development Campus, Diseases of the Developing World, GlaxoSmithKline, Tres Cantos, Madrid, Spain; ⁵Department of Chemistry and Applied Biosciences, Institute of Pharmaceutical Sciences, ETH Zürich, Switzerland; and ⁶Med.UL, Faculdade de Farmácia, Universidade de Lisboa, Portugal

Plasmodium parasites undergo a clinically silent and obligatory developmental phase in the host's liver cells before they are able to infect erythrocytes and cause malaria symptoms. To overcome the scarcity of compounds targeting the liver stage of malaria, we screened a library of 1037 existing drugs for their ability to inhibit *Plasmodium* hepatic development. Decoquinatone emerged as the strongest inhibitor of *Plasmodium* liver stages, both in vitro and in vivo. Furthermore, decoquinatone kills the parasite's replicative blood stages and is active against developing gametocytes, the forms responsible for transmission. The drug acts by selectively and specifically inhibiting the parasite's mitochondrial *bc₁* complex, with little cross-resistance with the antimalarial drug atovaquone. Oral administration of a single dose of decoquinatone effectively prevents the appearance of disease, warranting its exploitation as a potent antimalarial compound.

The search for active compounds among drugs originally developed and clinically tested for the treatment of other diseases is a particularly advantageous approach in the case of historically neglected diseases such as malaria. Although a number of reports have recently emerged where libraries of existing drugs were screened in the search for inhibitors of the malaria parasite *Plasmodium falciparum* [1–6], these screens have focused solely on the intraerythrocytic life cycle of *Plasmodium* infection, when clinical symptoms occur. However, the liver stage of *Plasmodium* infection is an obligatory step in the maturation and

replication of mosquito-delivered parasites toward generating the erythrocyte-infective forms that cause malaria symptoms [7]. To target the hepatic stage is therefore highly desirable in the context of malaria eradication, not only because its asymptomatic nature makes it ideally suited for prophylactic intervention [8], but also because the liver can serve as a reservoir for *Plasmodium vivax* and *Plasmodium ovale* hypnozoites, dormant parasite forms that may lead to relapses long after the initial blood infection has been eliminated [9]. In sharp contrast with drugs that kill blood-stage parasites, only a very limited number of drugs are available against liver forms. Among these, primaquine is the only clinically approved drug known to eliminate liver forms of *Plasmodium*, including hypnozoites, and to kill gametocytes, the sexual forms responsible for transmission of the parasite's life cycle inside the mosquito vector [10]. Despite primaquine's potentially lethal side effects that severely limit its use, except for a study from the 1980s [11], systematic efforts toward the identification of novel chemical safe entities efficacious against *Plasmodium* liver stages have not been reported [12]. Here, we describe the first screen targeted at *Plasmodium* liver stages and the identification of

Received 13 September 2011; accepted 23 November 2011; electronically published 6 March 2012.

Correspondence: Miguel Prudêncio, PhD, Unidade de Malária, Instituto de Medicina Molecular, Faculdade de Medicina, Universidade de Lisboa, Av. Prof. Egas Moniz, 1649-028 Lisboa, Portugal (mprudencio@fm.ul.pt).

The Journal of Infectious Diseases 2012;205:1278–86

© The Author 2012. Published by Oxford University Press on behalf of the Infectious Diseases Society of America. All rights reserved. For Permissions, please e-mail: journals.permissions@oup.com. This is an Open Access article distributed under the terms of the Creative Commons Attribution Non-Commercial License (<http://creativecommons.org/licenses/by-nc/3.0>), which permits unrestricted non-commercial use, distribution, and reproduction in any medium, provided the original work is properly cited.

DOI: 10.1093/infdis/jis184

decoquinatate, a compound that is shown to inhibit multiple phases of the parasite's life cycle. Further investigation revealed decoquinatate's mode of action and established its potential as a potent and selective antimalarial compound.

METHODS

Ethics Statement

All procedures involving animal models complied with European and US regulations.

Cells, Parasites, and Mice

Huh7 cells, a human hepatoma cell line, were cultured as described in the Supplementary Methods.

Two transgenic parasite lines were used in this study: a green fluorescent protein (GFP)-expressing *Plasmodium berghei* line (parasite line 259cl2) [13], as well as a fusion GFP- and firefly luciferase-expressing *P. berghei* line (parasite line 676m1cl1) (*PbGFP-Luc_{con}*) [14]. Sporozoites from both lines were freshly obtained through the disruption of salivary glands of infected female *Anopheles stephensi* mosquitoes.

Male C57Bl/6 mice aged 6–8 weeks and weighing 20–24 g were purchased from Charles River and housed in the pathogen-free facilities of the Instituto de Medicina Molecular (Lisbon, Portugal).

Drug Library Screen for Activity Against Malaria Liver Stages

Huh7 cells (1800 cells/well) were seeded in 30 μ L of complete Roswell Park Memorial Institute medium in 384-well collagen I coated plates (Greiner Bio-one) and incubated at 37°C with 5% CO₂. Forty-eight hours after seeding, prediluted drugs (5 μ L) were added to wells to achieve a final concentration of 10 μ M. After 1 hour, cells were infected with GFP-expressing *P. berghei* sporozoites (2000 sporozoites/well) freshly obtained through disruption of salivary glands of infected female *A. stephensi* mosquitoes. Twenty-four hours after infection, cells were fixed with 4% paraformaldehyde in phosphate-buffered saline (PBS) and permeabilized with 0.1% Triton X-100 in PBS, and cell nuclei were stained with Hoechst-33324 (Invitrogen).

Luminescence Measurement of In Vitro *Plasmodium* Infection

Inhibition of liver-stage infection was assessed by measuring the luminescence intensity of Huh-7 cells infected with a firefly luciferase-expressing *P. berghei* line, *PbGFP-Luc_{con}*, as previously reported [14].

Fluorescence-Activated Cell Sorting (FACS) Analysis

FACS analysis of cells infected with GFP-expressing parasites allows differentiation between the effect of a drug on hepatocyte invasion and on intrahepatocyte parasite development. FACS analysis at 2 and 48 hours after sporozoite addition was performed to determine the percentage of parasite-containing

cells and parasite-GFP intensity within infected cells. Cell samples for FACS analysis were processed as previously described [15].

In Vivo Drug-Efficacy Studies

All in vivo protocols were approved by the Animal Care Committee of the Instituto de Medicina Molecular and were performed according to the regulations of the European guidelines 86/609/EEG. Drug suspensions in soybean oil (200 μ L/mouse) or in an equivalent amount of vehicle were administered orally by gavage. Mice were infected by intravenous injection of 1×10^4 firefly luciferase-expressing *P. berghei* sporozoites. Alternatively, mice were infected by exposure to the bite of infected female *Anopheles stephensi* mosquitoes. Mosquitoes (20 per mouse) were allowed to feed for 30 minutes on mice anesthetized by intraperitoneal injection of 180 μ L of mixture consisting of 80 mg/kg of ketamine and 10 mg/kg xylazine dissolved in PBS.

Parasite load in the livers was determined 44–46 hours after infection by real-time in vivo imaging with the in vivo IVIS Lumina Imaging System [14]. Infection was allowed to proceed to the blood stage and was monitored by analysis of Giemsa-stained blood smears of tail blood collected between days 3 and 15 after infection. A compound was considered effective in the liver if, by day 15 after infection, no parasite could be detected in the blood smears.

Drug-Susceptibility Testing Against Asexual and Sexual Stages of 164/GFP Parasites

The drug-susceptibility assay was conducted as previously described [6]. Briefly, highly synchronized, young, ring-stage parasites in 110 μ L complete medium (4% hematocrit) were plated into 96-well plates (Microtest Tissue Culture Plates, Becton Dickinson) alongside uninfected red blood cells as a negative control. Sexual commitment was induced by a drop in hematocrit 24 hours after seeding the parasites. Serial dilutions of compounds were added at that point or 24 hours later, after reinvasion of parasites. Corresponding dilutions of chloroform were tested, as well, to account for solvent-specific effects. On the day of analysis, cells were stained with Hoechst, and cytometry data were collected as described in detail elsewhere [6]. These data were processed with Quanta software and were analyzed for half-maximal inhibitory concentrations (IC₅₀), using GraphPad Prism.

Ubiquinol-Cytochrome *bc₁* Oxidoreductase Activity

Ubiquinol-cytochrome *c* oxidoreductase activity was measured as the antimycin-sensitive decylubiquinol-cytochrome *c* oxidoreductase level in isolated mitochondria, as detailed in the Supplementary Methods.

Growth-Inhibition Assays for Evaluation of *bc₁* Inhibition

The sensitivity of *P. falciparum*-infected erythrocytes to various drugs was determined using a [³H]hypoxanthine incorporation

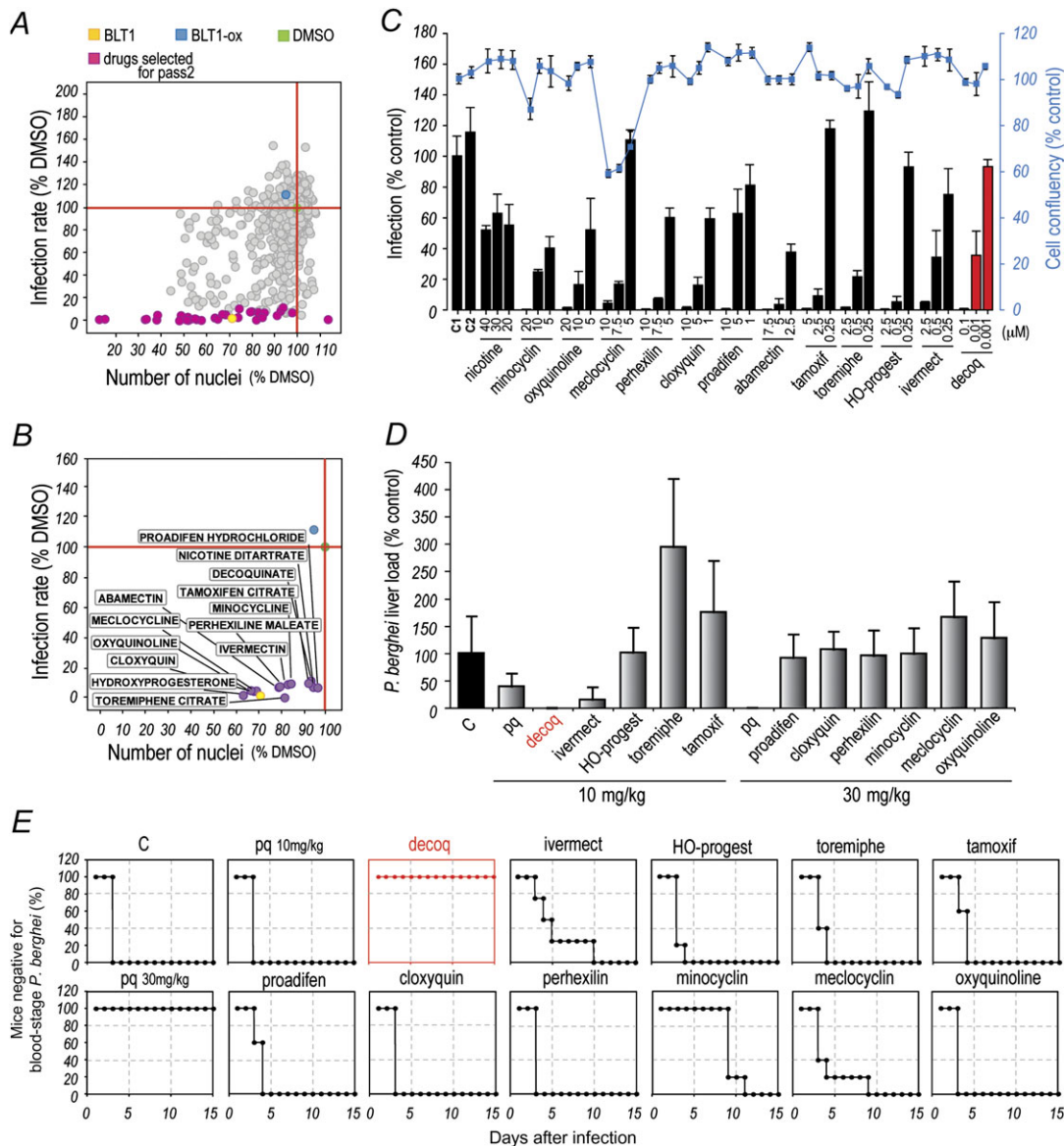


Figure 1. Screen of compound library. **A**, Results of the first screening round of 1037 compounds, highlighting the compounds leading to >90% decrease in infection. Blocker of lipid transport 1 (BLT-1) and its oxidized version (BLT-ox), previously used in the context of liver-stage *Plasmodium* infection [20], were used as positive and negative controls, respectively. **B**, Thirteen compounds selected after the second screening round. The plots in **A** and **B** depict the effect of the drugs on Huh7 cell proliferation (x-axis) and infection by *Plasmodium berghei* sporozoites (y-axis), measured 24 h after parasite addition. Each circle represents a compound. Green, yellow, and blue dots represent the dimethyl sulfoxide, positive control, and negative control, respectively, as above. The horizontal and vertical red lines indicate 100% infection and 100% confluency, respectively. **C**, Luminescence-based measurement of dose-dependent effects of selected compounds. Bars represent infection loads, and the red line represents cell confluency. Error bars represent SDs from 3 independent measurements. **D**, Luminescence-based measurements of liver parasite loads in mice following oral administration of selected compounds. Compounds were administered in the indicated amounts 24 h before, concomitantly with, and 24 h after intravenous injection of 10 000 luciferase-expressing *P. berghei* sporozoites. Error bars represent SDs ($n = 5$). **E**, Blood-stage patency of infection following oral administration of the same drugs as in **D**. Decoquinolate is highlighted in red in both **D** and **E**.

method with an inoculum size of 0.5% parasitemia and 2% hematocrit. Plates were incubated at 37°C in 5% CO₂, 5% O₂, and 95% N₂. After 24 hours of incubation, [³H]hypoxanthine was added and plates were incubated for an additional 24 hours. After that period, plates were harvested on a glass

fiber filter, using a TOMTEC Cell harvester 96. Filters were dried and melted on scintillator sheets, and the incorporated radioactivity was quantified by use of a Wallac Microbeta Trilux (Model 1450 LS- Perkin Elmer). The Dd2 cell line containing yeast dihydroorotate dehydrogenase (DHODH)

Table 1. Effect of Decoquinatone on Liver and Blood Stages of *Plasmodium* Infection, as Represented by Its Half-Maximal Inhibitory Concentration (IC₅₀)

Compound	Liver Stages (IC ₅₀)	Blood Stages (IC ₅₀)	
		Asexual	Sexual
Decoquinatone	2.6 ± 0.7	10 ± 8	36 ± 30
Primaquine	7500	11 000 ± 5000 [6]	No effect [6]
Artemisinin	NA	62 ± 14	92 ± 31
Atovaquone	NA	1.8 ± 0.2 [6]	Slight reduction [6]

IC₅₀ data are mean nM ± SD. Published IC₅₀ data given for comparison were taken from [6].
Abbreviation: NA, not available.

and its parental strain were cultured in the absence or presence of proguanil (1 μM). The *ScURA1* gene from *Saccharomyces cerevisiae* was amplified from genomic DNA and cloned into the pLN-14 vector. The *P. falciparum* Dd2attB strain was transfected by electroporation, and stable transfectants were selected with blasticidin. Both the Dd2attB_yeastDHODH strain and its parental strain, Dd2attB, were used in these assays. Nonlinear regression analysis was used to fit the normalized results of the dose-response curves, and IC₅₀ data were determined using the Grafit5 software package (Grafit program; Erithacus Software, Horley, Surrey, United Kingdom).

Molecular Modeling Studies

The molecular modeling studies were carried out using the crystal structure of cytochrome *bc*₁ from *S. cerevisiae* (PDB 3CX5) [16] as a template for generating the Y279S mutation. This was achieved using the Mutate Residue functionality within MOE (CCG MOE), which is an implementation of the method presented by Bower et al [17]. Mutant side-chain conformations are determined from a systematic rotamer search, resulting in acceptable side-chain structures that are based on the local environment. Docking was performed with the GOLD 5.01 (Genetic Optimization for Ligand Docking) package, which searches for the best ligand interaction pose, using a genetic algorithm. Docked ligands were ranked with GoldScore [18], which is included in the software, and were defined by the following components: protein-ligand hydrogen bond energy, protein-ligand van der Waals energy, ligand internal van der Waals energy, and ligand torsional strain energy. This fitness function has been optimized to predict the ligand-binding position and conformation of the ligands. Docking was run with standard settings and 1000 genetic algorithm operations. Atovaquone and decoquinatone were docked into the oxidation site in the targeted cytochrome. Visualization of best-fit docking poses was performed with

PyMOL after energy-minimization of the binding pocket and docked ligand with MOE (MMFF94x force field).

RESULTS

Chemical Screen Identifies Decoquinatone as a Potent Inhibitor of *Plasmodium* Liver Infection

We employed an in vitro infection model combining *P. berghei* parasites and the Huh7 human hepatoma cell line [15] to screen a commercially available library composed of 1037 compounds that have reached clinical stages (eg, clinical trials) in the United States (Supplementary Table 1) for their activity against *Plasmodium* liver stages. The high-throughput screen was carried out in a 384-well format combined with an automated microscopy high content readout (Supplementary Figure 1). The effect of each drug on the course of infection was assessed with the help of customized image analysis algorithms that allow for automatic quantification of both cell numbers and amount of intracellular parasites [19, 20]. The library was screened 3 independent times, using a fixed concentration of 10 μM of each compound. This process identified 116 compounds that decreased infection by >50% relative to the control. It is interesting to note that these compounds are distributed across a wide range of drug classes, suggesting a multiplicity of possible targets (Supplementary Figure 2). Among these compounds, the 41 producing a reduction in infection >90% were selected to undergo a second screening pass (Figure 1A and Supplementary Table 1), where their dose-response behavior was evaluated. On the basis of that response, and after exclusion of cytotoxic drugs, compounds with previously reported antiplasmodial activity, and topical drugs, 13 compounds were chosen to undergo a final round of in vitro screening (Figure 1A and 1B and Supplementary Table 1). In this assay, Huh7 cells and luciferase-expressing *P. berghei* parasites were used as previously described [14]. Each compound was assayed at 3 different concentrations, and their effects on infection load and cell confluence were evaluated by luminescence and fluorescence measurements, respectively. With the exception of nicotine, for which no dose-response was observed, all of the drugs led to a dose-dependent reduction in the *P. berghei* infection rate among Huh7 cells, albeit within different ranges of compound concentrations (Figure 1C). These results defined a final list of 12 compounds with proven in vitro activity against *Plasmodium* liver stages, which were selected for in vivo evaluation (Supplementary Table 1).

The ability of the selected compounds to inhibit infection in vivo was evaluated in an established rodent model of malaria. Mice received 3 treatments with 10 or 30 mg/kg of each compound, administered orally 24 hours before, concomitantly with, and 24 hours after intravenous injection of 10 000 luciferase-expressing *P. berghei* sporozoites. Liver parasite burdens

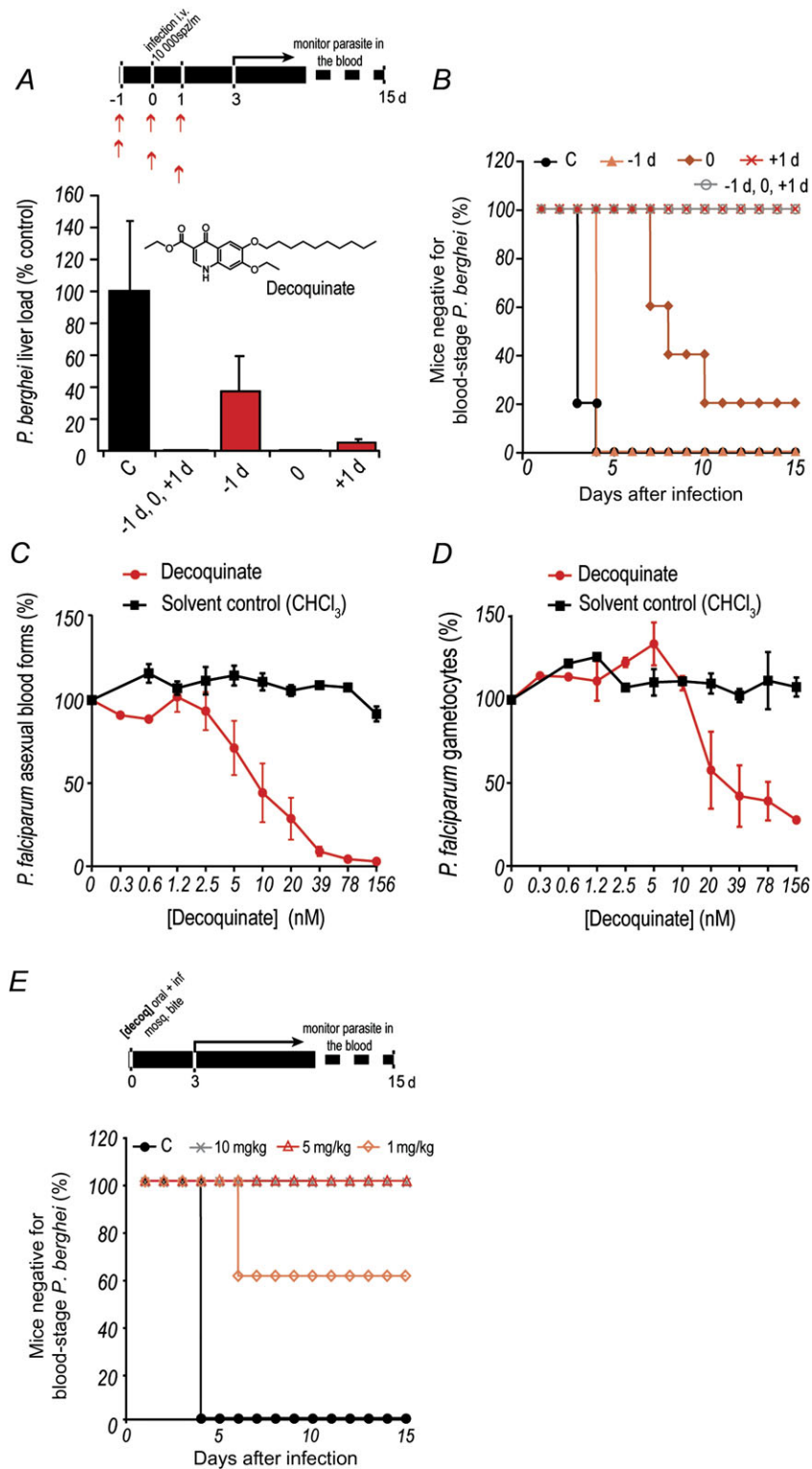


Figure 2. Inhibition of *Plasmodium* by decoquinatone. *A, B*, Oral administration of 10 mg/kg of decoquinatone at various times relative to intravenous injection of 10 000 luciferase-expressing *Plasmodium berghei* sporozoites. Luminescence-based measurement of liver parasite loads are shown in *A*, and blood-stage patency of infection is shown in *B*. The inset depicts the structure of the decoquinatone molecule. Results shown are representative from 3 independent experiments. Error bars represent SDs (n = 5). *C, D*, Half-maximal inhibitory concentration curves representing the effect of decoquinatone on parasite (*C*) and gametocyte (*D*) load. Each assay represents at least 3 biological replicates with 2 technical replicates per plate. The graphs show mean values of the experiments, whereas the error bars represent the standard error of the mean. *E*, Blood-stage patency of infection in mice following oral administration of a single dose of decoquinatone immediately prior to *P. berghei* sporozoite delivery by mosquito bite (n = 5). Abbreviation: C, control.

Table 2. Sensitivity of Ubiquinol:Cytochrome *bc*₁ Activity to Decoquinatate and Atovaquone on Isolated Mitochondria

Ubiquinol Cytochrome <i>c</i> Reductase	IC ₅₀ (mean μM ± SD)	
	Decoquinatate	Atovaquone
<i>P. falciparum</i>	0.002 ± 0.0005	0.0002 ± 0.00003
HEK293	>10	0.327 ± 0.03

Abbreviation: *P. falciparum*, *Plasmodium falciparum*.

were determined by luminescence 44 hours after infection (Figure 1D), and blood parasitemias were monitored daily for 15 days (Figure 1E). Most notably, decoquinatate consistently emerged from our studies as the most potent inhibitor of *Plasmodium* infection in vivo, completely abrogating liver parasitemia and fully preventing the appearance of parasites in the blood at 10 mg/kg. Decoquinatate's IC₅₀ against liver stages in vitro was estimated at 2.6 nM, approximately 3000-fold lower than that of primaquine (Table 1 and Supplementary Figure 3A). Flow cytometry analysis of Huh7 cells infected with GFP-expressing *P. berghei* sporozoites further demonstrated that decoquinatate acts by inhibiting *Plasmodium*'s intracellular replication, rather than its ability to invade hepatic cells (Supplementary Figure 3B).

Decoquinatate Acts on Asexual and Presexual *Plasmodium* Blood Forms

We then investigated the degree of protection conferred by different decoquinatate administration schedules relative to parasite inoculation. To this end, the drug was administered orally to mice at 10 mg/kg, at different times relative to intravenous injection of 10 000 luciferase-expressing sporozoites (Figure 2A). Our results showed that administration of decoquinatate in any of these schedules significantly decreased parasite liver load, compared with untreated controls (Figure 2A). Interestingly, liver parasite load decreased to below detectable levels in mice treated immediately prior to infection, but they eventually developed blood parasitemia, although significantly delayed ($P = .00159$), while mice treated 24 hours after infection remained negative for blood-stage parasites (Figure 2B). This suggests that decoquinatate acts not only on *Plasmodium* liver stages but also on the blood forms of the parasite. To confirm this, the effect of decoquinatate on in vitro cultures of *P. falciparum* strain 164/GFP blood stages was evaluated using methods described elsewhere [6] (Figure 2C and Table 1). Indeed, decoquinatate displayed a marked effect on asexual blood stages of *Plasmodium*, with an IC₅₀ of the same order of magnitude of that of artemisinin, an effective blood schizonticidal antimalarial, and approximately 1000-fold lower than that of primaquine. Crucially, our data also showed that decoquinatate is active against *Plasmodium* gametocytes, the

presexual blood forms of the parasite responsible for transmission to the invertebrate host, with an IC₅₀ of 36 nM (Figure 2D and Table 1).

Finally, we sought to establish the minimal decoquinatate dose that would provide complete protection against infection transmitted to mice by mosquito bite, the most physiologically relevant transmission route. A single decoquinatate dose of 10, 5, or 1 mg/kg was administered orally prior to sporozoite injection by *P. berghei*-infected mosquitoes, followed by daily monitoring of blood parasitemia. Results showed that whereas 1 mg/kg of decoquinatate could already confer partial protection, a single 5 mg/kg dose of the compound completely prevented the appearance of blood-stage parasites (Figure 2E).

Decoquinatate Specifically and Selectively Inhibits *Plasmodium* Mitochondrial *bc*₁ Complex

Given the structural similarities with other quinolones known to inhibit *Plasmodium*'s cytochrome *bc*₁ complex (ubiquinol:cythochrome *c* oxidoreductase or respiratory complex III; *bc*₁; *P. falciparum* genes 2655541, 811955) [21], we investigated whether the mechanism of decoquinatate's antimalarial activity could be explained by *bc*₁ inhibition. To address this, we initially assessed decoquinatate inhibition of *bc*₁ activity on mitochondria isolated from *P. falciparum* 3D7A parasites and human HEK293 cells. We found plasmodial *bc*₁ complex to be susceptible to decoquinatate, with an IC₅₀ of 0.002 μM and a selectivity index of >5000, when compared with its human counterpart (Table 2). To confirm the antimalarial mode of action of decoquinatate by inhibition of *bc*₁ complex, we then carried out a series of growth inhibition experiments (Figure 3). The mitochondrial electron transport chain (ETC) is critical for parasite survival, inhibition of the *P. falciparum* cytochrome *bc*₁ being the mode of action of the antimalarial drug atovaquone [22] (Figure 3A). ETC is used by *Plasmodium* as the only way to regenerate mitochondrial coenzyme Q. This is the electron receptor used by DHODH, a mitochondrion-located, membrane-anchored enzyme of the pyrimidine biosynthetic pathway. DHODH is also essential for survival because *Plasmodium* cannot salvage pyrimidines [23] (Figure 3A). Artemisinin, a known potent antimalarial, kills the parasite by a different mechanism, presumably one involving hemoglobin digestion [24], and can therefore be used as an appropriate control for assays to measure the mode of action of growth inhibition. We showed that *P. falciparum* growth was effectively inhibited by decoquinatate, atovaquone, a specific DHODH inhibitor, and artemisinin (Figure 3B–E and Table 3). These drugs were then assayed on a *P. falciparum* strain transfected with cytoplasmic *S. cerevisiae* DHODH (ScDHODH), which bypasses the endogenous *Plasmodium* counterpart that is required for pyrimidine biosynthesis. ScDHODH uses fumarate instead of mitochondrial coenzyme Q as an electron acceptor, and therefore the transgenic strain

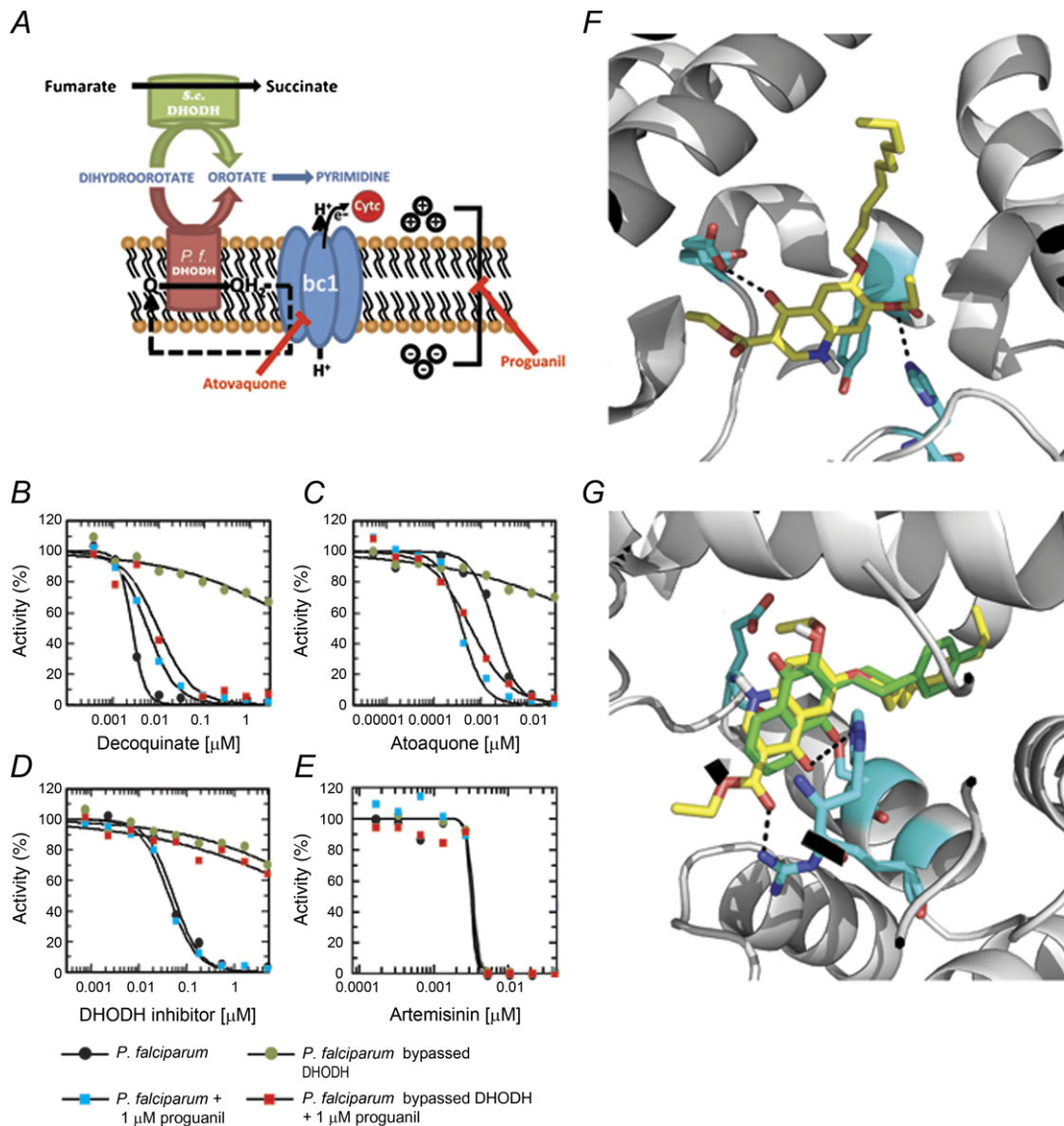


Figure 3. Antiplasmodial mode of action of decoquinatate. *A*, Generation of *P. falciparum* mitochondrial membrane potential by *bc*₁ complex-mediated and dihydroorotate dehydrogenase (DHODH)-mediated reactions. *Plasmodium falciparum* (*P. f.*) DHODH is the key enzyme in the reduction of coenzyme Q (from Q to QH₂). QH₂ is reoxidized by the *bc*₁ complex with subsequent electron transfer to cytochrome *c*, resulting in proton translocation and generation of electropotential across the inner membrane. Inhibitors of the *bc*₁ complex prevent this mode of electropotential generation, as well as reoxidation of QH₂. In this scenario, pyrimidine synthesis can be secured by *Saccharomyces cerevisiae* DHODH, which bypasses plasmodial DHODH by using fumarate as the electron acceptor, while a proguanil-sensitive alternate path can provide the necessary membrane potential. Thus, in the presence of atovaquone or other electron transport inhibitors, the generation of electropotential becomes hypersensitive to proguanil (adapted from [18]). *B–E*, *P. falciparum* in vitro growth curves and genetic rescue with yeast DHODH. Addition of proguanil restores sensitivity of the *P. falciparum* line with *S. cerevisiae* DHODH to decoquinatate and atovaquone but not to a specific DHODH inhibitor. Artemisinin is used as a *bc*₁ complex-independent and DHODH-independent control for growth inhibition. *F*, Docking pose of decoquinatate for the wild-type *bc*₁ complex. A hydrogen bond with H181 and a carbonyl-carbonyl interaction with E272 are established between protein and ligand. *G*, Docking poses of ligands for the mutant cytochrome *bc*₁ model. Decoquinatate is represented in yellow and atovaquone in green. Decoquinatate is within hydrogen bond distance of H181 and R283, whereas atovaquone loses the ability to interact with E272 and H181.

is resistant to both *bc*₁ and DHODH inhibitors [23]. This *Plasmodium* strain remained sensitive to artemisinin but was not killed by decoquinatate, atovaquone, or the DHODH inhibitor, suggesting that the latter 3 compounds block pyrimidine biosynthesis (Figure 3*B–E* and Table 3). Finally, to

distinguish *bc*₁ from DHODH inhibition, the assay was performed in the presence of proguanil, which collapses the mitochondrial membrane potential when electron transport is inhibited and renders the ScDHODH-expressing strain sensitive to ETC inhibitors [23]. Addition of proguanil restored inhibition

Table 3. Growth Inhibition of Parental and Transgenic *Plasmodium falciparum* Strains in the Absence or Presence of Proguanil

Parasite Strain	Proguanil (1 μ M)	IC ₅₀ (mean μ M \pm SD)			
		Decoquinatate	DHODH Inhibitor	Atovaquone	Artemisinin
Dd2attB	Absent	0.003 \pm 0.0001	0.046 \pm 0.006	0.002 \pm 0.00002	0.004 \pm 0.0008
Dd2attB	Present	0.006 \pm 0.0004	0.048 \pm 0.002	0.0004 \pm 2 \times 10 ⁻⁵	0.004 \pm 0.0008
Dd2attB_yeastDHODH	Absent	>2.5	>5	>0.035	0.004 \pm 0.0008
Dd2attB_yeastDHODH	Present	0.011 \pm 0.001	>5	0.001 \pm 7.5 \times 10 ⁻⁵	0.003 \pm 4 \times 10 ⁻⁵

by decoquinatate and atovaquone but not by the DHODH inhibitor (Figure 3B–E and Table 3). Overall, these results show that decoquinatate's antimalarial mode of action is the potent, selective, and specific inhibition of *P. falciparum* mitochondrial *bc*₁ complex.

Decoquinatate Presents Little Cross-Resistance With Atovaquone

Resistance to atovaquone, presently the only drug in clinical use that targets *bc*₁, emerged rapidly [25]. This raised the need for alternative *bc*₁ inhibitors with little cross-resistance with atovaquone-resistant strains, as is the case of quinolones [21]. The fact that, unlike atovaquone [6], decoquinatate shows potent gametocidal activity indicated that the 2 drugs interact differently with their *bc*₁ complex target. To further predict whether decoquinatate presents cross-resistance with atovaquone, we carried out a molecular docking study that used *S. cerevisiae* *bc*₁ complex structure (PDB 3CX5) [16] as a surrogate for the *P. falciparum* protein. This approach has been used effectively to study the binding mode of atovaquone, given the high sequence identity at the Q_o site of cytochrome *b* [26]. Decoquinatate presented a similar docking pose to 4(1*H*)-pyridones in the wild-type protein [27], which is consistent with its IC₅₀ (Figure 3F). The Y279S mutation (yeast numbering) corresponds to one of the most frequent mutations in *P. falciparum* and results in resistance to atovaquone [26]. Molecular-docking runs on a mutated model generated from 3CX5 showed that Y279 is critical for atovaquone binding, as mutation to S279 (Figure 3G) leads to loss of interaction with E272 and H181 [27, 28]. Introduction of the Y279S mutation led to inversion in the docking pose of decoquinatate. However, the protein-inhibitor complex is still stabilized by hydrogen bonds with H181 and R283 and by hydrophobic interactions with residues from the binding pocket (Figure 3G). Therefore, decoquinatate is expected to inhibit the Y279S mutant of cytochrome *bc*₁ effectively and is therefore expected to present little cross-resistance with atovaquone. This prediction was confirmed in a very recent report that showed that decoquinatate indeed possesses limited cross-resistance against 5 atovaquone-resistant *P. falciparum* lines [29].

DISCUSSION

Decoquinatate is a cheap and widely available coccidiostat commonly used in livestock ranging from poultry to mammals [30]

and has been recently identified in a screen for blood-stage inhibitors of *Plasmodium* infection [29]. The data presented here demonstrate that decoquinatate is a potent antimalarial, with transmission blocking potential due to the marked effect on various stages of *Plasmodium*'s life cycle. Its identification stemmed from the first high-throughput, microscopy-based screen performed to identify compounds that inhibit the hepatic stage of plasmodial infection. Besides its ability to inhibit the development of the parasite's liver stages, decoquinatate demonstrated strong activity against *Plasmodium* blood forms, including gametocytes, which are latent pre-sexual parasite forms responsible for the transmission of *Plasmodium* to *Anopheles* mosquitoes. This is in contrast with atovaquone, which has been shown to present activity against *Plasmodium* liver stages [31] but to be only slightly effective against parasites in the early sexual stage [6]. Importantly, a previous study has concluded that compounds shown to be gametocytocidal also possess radical curative effects against true relapsing malaras [32]. Thus, although the present study does not provide direct evidence for this, decoquinatate's strong effect against latent gametocytes suggests that it might be active against hypnozoites, which are latent parasite forms in the liver. On the other hand, drugs targeting multiple stages of *Plasmodium*'s life cycle may present added advantages in terms of efficacy. Decoquinatate inhibits the *bc*₁ complex, an important, yet underexploited antimalarial target. The rapid emergence of resistance to atovaquone led to its combination with proguanil (Malarone), the cost of which limited its widespread use in resource-poor, disease-endemic areas and highlighted the need for cheaper alternatives that can overcome resistance [21]. Given its little cross-resistance with atovaquone-resistant strains [29], decoquinatate may constitute one such alternative. In this context, and at a time when novel drugs against malaria are urgently required, this study paves the way not only for future screening efforts of a similar nature but also for further exploitation of decoquinatate as part of an antimalarial strategy.

Supplementary Data

Supplementary materials are available at The Journal of Infectious Diseases online (http://www.oxfordjournals.org/our_journals/jid/). Supplementary materials consist of data provided by the author that are published to benefit the reader. The posted materials are not copyedited. The contents

of all supplementary data are the sole responsibility of the authors. Questions or messages regarding errors should be addressed to the author.

Notes

Acknowledgments. F. P. C. acknowledges FCT for postdoctoral grant BPD/64539/2010. K. B. acknowledges a postdoctoral Feodor Lynen fellowship from the Alexander von Humboldt foundation. T. R. was supported by the Chemical Computing Group, which provided a research license to ETH for the use of MOE. M. M. M. is a Howard Hughes Medical Institute International Scholar. M. P. is a holder of a Ciência 2007 position of the Portuguese Ministry of Science.

Financial support. This work was supported by Fundação para a Ciência e Tecnologia (grant PTDC/SAU-MII/099118/2008 to M P; grants PTDC/SAU-GMG/100313/2008 and HMSP-CT/SAU-ICT/10068/2009 to M M M), by the NGFN Transfer program of the German Ministry of Education and Research, and by the European Union's Framework Programme 7 (grant 242095 to M M M). This work was developed under the scope of EVIMalaR (EC-FP7).

Potential conflicts of interest. All authors: No reported conflicts.

All authors have submitted the ICMJE Form for Disclosure of Potential Conflicts of Interest. Conflicts that the editors consider relevant to the content of the manuscript have been disclosed.

References

1. Yuan J, Cheng KC, Johnson RL, et al. Chemical genomic profiling for antimalarial therapies, response signatures, and molecular targets. *Science* **2011**; 333:724–9.
2. Chong CR, Chen X, Shi L, Liu JO, Sullivan DJ Jr. A clinical drug library screen identifies astemizole as an antimalarial agent. *Nat Chem Biol* **2006**; 2:415–16.
3. Guiguemde WA, Shelat AA, Bouck D, et al. Chemical genetics of *Plasmodium falciparum*. *Nature* **2010**; 465:311–15.
4. Gamo FJ, Sanz LM, Vidal J, et al. Thousands of chemical starting points for antimalarial lead identification. *Nature* **2010**; 465:305–10.
5. Rush MA, Baniecki ML, Mazitschek R, et al. Colorimetric high-throughput screen for detection of heme crystallization inhibitors. *Antimicrob Agents Chemother* **2009**; 53:2564–8.
6. Buchholz K, Burke TA, Williamson KC, Wiegand RC, Wirth DF, Marti M. A high-throughput screen targeting malaria transmission stages opens new avenues for drug development. *J Infect Dis* **2011**; 203:1445–53.
7. Prudencio M, Rodriguez A, Mota MM. The silent path to thousands of merozoites: the *Plasmodium* liver stage. *Nat Rev Microbiol* **2006**; 4:849–56.
8. Mazier D, Renia L, Snounou G. A pre-emptive strike against malaria's stealthy hepatic forms. *Nat Rev Drug Discov* **2009**; 8:854–64.
9. Wells TN, Burrows JN, Baird JK. Targeting the hypnozoite reservoir of *Plasmodium vivax*: the hidden obstacle to malaria elimination. *Trends Parasitol* **2010**; 26:145–51.
10. Vale N, Moreira R, Gomes P. Primaquine revisited six decades after its discovery. *Eur J Med Chem* **2009**; 44:937–53.
11. Davidson DE Jr, Ager AL, Brown JL, Chapple FE, Whitmire RE, Rossan RN. New tissue schizontocidal antimalarial drugs. *Bull World Health Organ* **1981**; 59:463–79.
12. Prudencio M, Mota MM, Mendes AM. A toolbox to study liver stage malaria. *Trends Parasitol* **2011**; 27:565–574.
13. Franke-Fayard B, Trueman H, Ramesar J, et al. A *Plasmodium berghei* reference line that constitutively expresses GFP at a high level throughout the complete life cycle. *Mol Biochem Parasitol* **2004**; 137:23–33.
14. Ploemen IH, Prudencio M, Douradinha BG, et al. Visualisation and quantitative analysis of the rodent malaria liver stage by real time imaging. *PLoS One* **2009**; 4:e7881.
15. Prudencio M, Rodrigues CD, Ataíde R, Mota MM. Dissecting in vitro host cell infection by *Plasmodium* sporozoites using flow cytometry. *Cell Microbiol* **2008**; 10:218–24.
16. Solmaz SR, Hunte C. Structure of complex III with bound cytochrome c in reduced state and definition of a minimal core interface for electron transfer. *J Biol Chem* **2008**; 283:17542–9.
17. Bower MJ, Cohen FE, Dunbrack RL Jr. Prediction of protein side-chain rotamers from a backbone-dependent rotamer library: a new homology modeling tool. *J Mol Biol* **1997**; 267:1268–82.
18. Jones G, Willett P, Glen RC, Leach AR, Taylor R. Development and validation of a genetic algorithm for flexible docking. *J Mol Biol* **1997**; 267:727–48.
19. Prudencio M, Rodrigues CD, Hannus M, et al. Kinome-wide RNAi screen implicates at least 5 host hepatocyte kinases in *Plasmodium* sporozoite infection. *PLoS Pathog* **2008**; 4:e1000201.
20. Rodrigues CD, Hannus M, Prudencio M, et al. Host scavenger receptor SR-BI plays a dual role in the establishment of malaria parasite liver infection. *Cell Host Microbe* **2008**; 4:271–82.
21. Barton V, Fisher N, Biagini GA, Ward SA, O'Neill PM. Inhibiting *Plasmodium* cytochrome bc1: a complex issue. *Curr Opin Chem Biol* **2010**; 14:440–6.
22. Fry M, Pudney M. Site of action of the antimalarial hydroxynaphthoquinone, 2-[trans-4-(4'-chlorophenyl) cyclohexyl]-3-hydroxy-1, 4-naphthoquinone (566C80). *Biochem Pharmacol* **1992**; 43:1545–53.
23. Painter HJ, Morrissey JM, Mather MW, Vaidya AB. Specific role of mitochondrial electron transport in blood-stage *Plasmodium falciparum*. *Nature* **2007**; 446:88–91.
24. Klonis N, Crespo-Ortiz MP, Bottova I, et al. Artemisinin activity against *Plasmodium falciparum* requires hemoglobin uptake and digestion. *Proc Natl Acad Sci U S A* **2011**; 108:11405–10.
25. Looareesuwan S, Viravan C, Webster HK, Kyle DE, Hutchinson DB, Canfield CJ. Clinical studies of atovaquone, alone or in combination with other antimalarial drugs, for treatment of acute uncomplicated malaria in Thailand. *Am J Trop Med Hyg* **1996**; 54:62–6.
26. Kessl JJ, Ha KH, Merritt AK, et al. Cytochrome b mutations that modify the ubiquinol-binding pocket of the cytochrome bc1 complex and confer anti-malarial drug resistance in *Saccharomyces cerevisiae*. *J Biol Chem* **2005**; 280:17142–8.
27. Rodrigues T, Guedes RC, dos Santos DJ, et al. Design, synthesis and structure-activity relationships of (1H-pyridin-4-ylidene)amines as potential antimalarials. *Bioorg Med Chem Lett* **2009**; 19:3476–80.
28. Kessl JJ, Lange BB, Merbitz-Zahradnik T, et al. Molecular basis for atovaquone binding to the cytochrome bc1 complex. *J Biol Chem* **2003**; 278:31312–18.
29. Nam TG, McNamara CW, Bopp S, et al. A chemical genomic analysis of decoquinone, a *Plasmodium falciparum* cytochrome b inhibitor. *ACS Chem Biol* **2011**.
30. Dorne JL, Fernandez-Cruz ML, Bertelsen U, et al. Risk assessment of coccidiostats during feed cross-contamination: animal and human health aspects. *Toxicol Appl Pharmacol* **2011**.
31. Davies CS, Pudney M, Nicholas JC, Sinden RE. The novel hydroxynaphthoquinone 566C80 inhibits the development of liver stages of *Plasmodium berghei* cultured in vitro. *Parasitology* **1993**; 106:1–6.
32. Gwadz RW, Koontz LC, Miller LH, Davidson DE Jr. *Plasmodium gallinaceum*: avian screen for drugs with radical curative properties. *Exp Parasitol* **1983**; 55:188–96.